Inorganic Chemistry

Communication

pubs.acs.org/IC

New Layered Iron Sulfide $NaFe_{1.6}S_2$: Synthesis and Characterization

Xiaofang Lai, Xiaolong Chen,* Shifeng Jin, Gang Wang, Tingting Zhou, Tianping Ying, Han Zhang, Shijie Shen, and Wanyan Wang

Research & Development Center for Functional Crystals, Beijing National Laboratory for Condensed Matter Physics, Institute of Physics, Chinese Academy of Sciences, P.O. Box 603, Beijing 100190, China

Supporting Information

ABSTRACT: Na was intercalated between $[Fe_2S_2]$ layers for the first time, giving a novel compound $NaFe_{1.6}S_2$. This material adopts a $CaAl_2Si_2$-type structure with ~20% iron vacancies and represents the first layered compound in a ternary Na−M−X (M = Fe, Co, Ni; X = S, Se) system. First-principles calculations reveal that phonon dynamics is an important factor for it to prefer the $CaAl_2Si_2$-type rather than the $ThCr_2Si_2$-type structure. It features a magnetic transition at 205 K and is a narrow-band-gap semiconductor.

Layered iron-based compounds have been of great interest because of their fascinating properties, such as high-temperature superconductivity and intimate correlation between superconductivity and antiferromagnetism.[1] Up to now, there have been at least four structure types of FeAs-based superconductors,[2] all consisting of alternate stacking of antifluorite-like $[Fe_2As_2]^{2-}$ layers and spacer layers, typically, alkali- or alkaline-metal cations,[3] fluorite-like $[La_2O_2]^{2+}$ or $[Ca_2F_2]^{2+}$ layers,[4] or more complex $[Sr_4V_2O_6]^{2+}$ blocks.[5] The structural diversity not only confirms that superconductivity arises in the $[Fe_2As_2]^{2-}$ layer but also reveals that the $[Fe_2As_2]^{2-}$ layer is sufficiently flexible to match well with a variety of spacer layers. Similar to the $[Fe_2As_2]^{2-}$ layer, the antifluorite-like $[Fe_2Ch_2]$ (Ch = Se, Te) layer can also be responsible for superconductivity.[6] However, the number of the intercalated compounds of the $[Fe_2Ch_2]$ layers has been rather limited up to now.

Recently, superconductivity at around 30 K was found in the $ThCr_2Si_2$-type $A_xFe_{2-y}Se_2$ (A = alkali metal or Tl) and $K_xFe_{2-y}SeS$.[7] This has renewed interest in the iron-based superconductors as well as in the structurally related $A_xM_{2-y}X_2$ (A = alkali metal or Tl; M = Fe, Co, Ni; X = S, Se) system, which has been studied decades ago and known to exhibit interesting magnetic properties.[8] In contrast to K, Rb, Cs, and Tl, the smaller alkali-metal Na is difficult to intercalate between $[Fe_2Se_2]$ layers by a conventional solid-state reaction method. Huang et al. reported Na intercalation between $[Fe_2Se_2]$ layers, but the content of Na is low ($Na_{0.1}Fe_2Se_2$) and the structure remains the same as FeSe.[9] Interestingly, Na can be intercalated between $[Fe_2Se_2]$ layers by a liquid ammonia method,[10] but experiments suggest that between $[Fe_2Se_2]$ layers there are ammonia molecules that play an important role in stabilizing the structure of the obtained superconducting compound $Na_x(NH_3)_yFe_2Se_2$.[11] So, it remains an open question whether Na alone can be intercalated between other $[M_2X_2]$ except $[Fe_2Se_2]$ layers. Here, we report the synthesis and characterization of new layered iron sulfide $NaFe_{1.6}S_2$. It adopts a $CaAl_2Si_2$-type rather than a $ThCr_2Si_2$-type structure, featuring a novel type of hexagonal $Fe_{1.6}S_2$ layer. First-principles calculations reveal that the $CaAl_2Si_2$-type structure is dynamically stable, while the $ThCr_2Si_2$-type structure is not. Magnetic, heat capacity, and electrical measurements show that $NaFe_{1.6}S_2$ is a magnetic semiconductor.

A series of $Na_xFe_{2-y}S_{2+z}$ ($0.8 \le x \le 1$, $0.3 \le y \le 0.6$, $0 \le z \le 0.1$) samples have been prepared by the direct reaction of Na lumps and Fe and S powders (for details for the synthesis and characterization, see the Supporting Information, SI). However, we found that only the samples with $NaFe_{1.6}S_2$ composition were relatively pure [comparison of the powder X-ray diffraction (PXRD) patterns for all compositions; Figure S1, SI]. For clarity, we discuss the properties of the $NaFe_{1.6}S_2$ composition only. The obtained $NaFe_{1.6}S_2$ polycrystals were dark black and extremely air-sensitive, so great care was taken in specimen preparation for characterization. The room temperature PXRD data (including a little FeS impurity, about 2 wt %) were well indexed based on a trigonal cell with lattice parameters a = 3.8557(3) Å and c = 6.7928(7) Å. The structure of $CaAl_2Si_2$[12] was used as a starting model for the Rietveld refinement against the raw data. Shown in Figure 1a are the final Rietveld refinement profiles, with agreement factors R_p = 2.66%, R_{wp} = 3.42%, and χ^2 = 2.01. The refined structure parameters are summarized in Table 1.

The average atomic ratios Na:Fe:S = 0.978(15):1.558(26):2 determined from a PXRD fitting are close to those obtained by inductively coupled plasma atomic emission spectrometry (ICP-AES): Na:Fe:S = 0.98(1):1.57(2):2.0(1). Just like a $K_xFe_{2-y}Se_2$ superconductor,[7a] here the $Fe_{1.6}S_2$ layers are also not completely filled: with about 20% iron vacancies, possibly a direct consequence of charge balance. Illustrated in the inset of Figure 1a is the crystal structure of $NaFe_{1.6}S_2$, in which two-dimensional rafts of Na^+ ions are separated by hexagonal $Fe_{1.6}S_2$ layers. The $Fe_{1.6}S_2$ layer is made of FeS_4 tetrahedra, which are as regular as those MX_4 in other $A_xM_{2-y}X_2$ and Na−M−X compounds,[7,8,13] except that the difference among the Fe−S bonds is bigger [2.372(2) Å × 3 and 2.383(7) Å × 1, where the difference is 0.011 Å]. Different from the case in other $A_xM_{2-y}X_2$ compounds, here the Fe atoms of the $Fe_{1.6}S_2$ layer are not in the same plane perpendicular to the c axis but form two atomic planes slightly staggered along the c axis (1.56 Å apart). As shown in Figure 1b, in the hexagonal $Fe_{1.6}S_2$ layer of $NaFe_{1.6}S_2$, each FeS_4 tetrahedron shares an edge with the three neighboring FeS_4 tetrahedra,

Received: June 29, 2013
Published: October 25, 2013

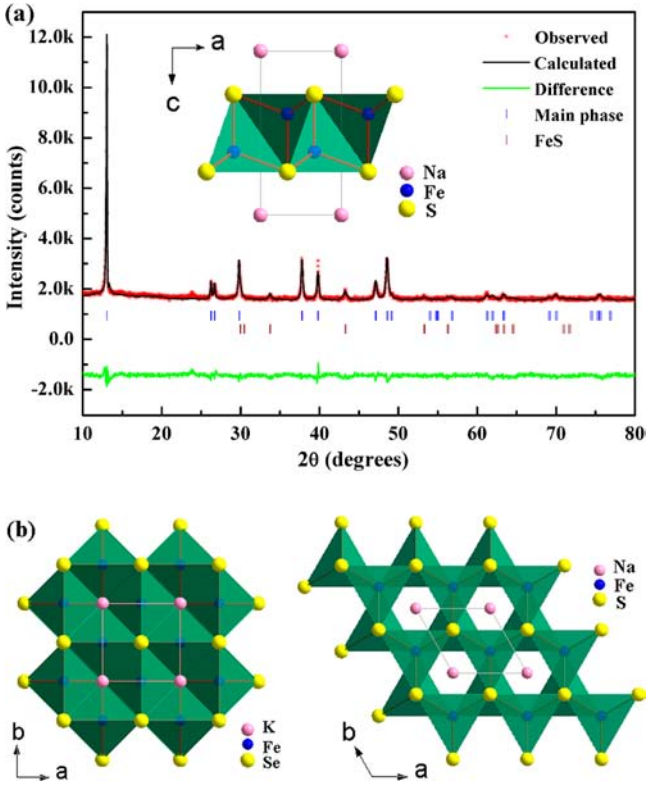

Figure 1. (a) PXRD pattern collected for a nominal $NaFe_{1.6}S_2$ sample and the Rietveld refinement profiles. The inset shows the schematic crystal structure of $NaFe_{1.6}S_2$ ($CaAl_2Si_2$ type). (b) Comparison of the structures of $K_xFe_{2-y}Se_2$ (left side) and $NaFe_{1.6}S_2$ (right side) viewed down [001], with $FeSe_4$ and FeS_4 tetrahedra shown in green.

Table 1. Crystallographic Data of $NaFe_{1.6}S_2$[a]

atom	x	y	z	occupancy
Na	0	0	0	0.978(15)
Fe	$^1/_3$	$^2/_3$	0.3848(6)	0.779(13)
S	$^2/_3$	$^1/_3$	0.2644(8)	1

[a]Space group $P\bar{3}\,m1$, $a = b = 3.8557(3)$ Å, and $c = 6.7928(7)$ Å.

resulting in a layer with octahedral cavities, while in the tetrahedral $M_{2-y}X_2$ layer of other $A_xM_{2-y}X_2$ compounds, take $K_xFe_{2-y}Se_2$[7a] for example, each $FeSe_4$ tetrahedron shares an edge with the four neighboring $FeSe_4$ tetrahedra, thus forming a layer without cavities. For most of the Na−M−X compounds, the MX_4 tetrahedra are usually found to be discrete or linked by an edge and/or a corner, producing infinite chains or columns,[13] and $NaFe_{1.6}S_2$ is the first example of MX_4 tetrahedra sharing an edge to form two-dimensional layers, although with cavities. For $NaFe_{1.6}S_2$, Na cations are 6-coordinated rather than 8-coordinated by S anions, on a position just above the octahedral cavity in the $Fe_{1.6}S_2$ layer, with much shorter Na−S bonds. It is probably this geometry that stabilizes the structure.

$NaFe_{1.6}S_2$ is a novel example in both $A_xM_{2-y}X_2$ and Na−M−X systems, in that (I) Na was originally thought to be difficult to insert between $[M_2X_2]$ layers, (II) a $CaAl_2Si_2$-type structure is without precedent in the $A_xM_{2-y}X_2$ system, and (III) layers of edge-shared MX_4 tetrahedra are rare in the NaMX system. On the basis of these characters, we elucidate the structural peculiarity by assessing the stabilities of a hypothetical $ThCr_2Si_2$-type $NaFe_{1.6}S_2$ (crystallographic data are taken to be similar to those of $K_xFe_{2-y}S_2$[14]) and the $CaAl_2Si_2$-type $NaFe_{1.6}S_2$ via first-principles calculations (for calculation details, see the SI). The calculated energy of the $ThCr_2Si_2$-type structure (−3594.23 eV/formula) is 650 meV lower than that of the $CaAl_2Si_2$-type structure (−3593.58 eV/formula). However, the $ThCr_2Si_2$-type structure is dynamically unstable, as discussed below. The phonon dispersion curves calculated along the high-symmetry lines of the Brillouin zone and the corresponding partial densities of the phonon states of $NaFe_{1.6}S_2$ with $ThCr_2Si_2$- and $CaAl_2Si_2$-type structures are shown in Figure 2. For the $ThCr_2Si_2$-type

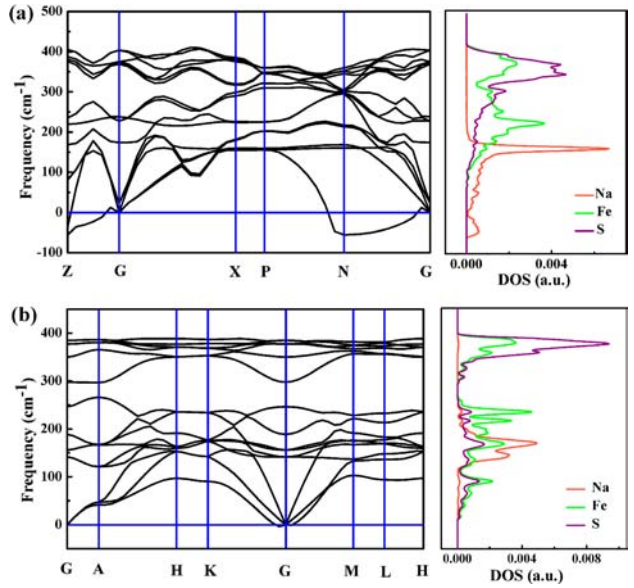

Figure 2. Phonon dispersion relations and partial densities of the phonon states of (a) hypothetical $ThCr_2Si_2$-type $NaFe_{1.6}S_2$ and (b) synthetic $CaAl_2Si_2$-type $NaFe_{1.6}S_2$.

structure, there are soft modes (negative frequencies) along the Z−G, P−N, and N−G directions, mainly due to the vibration of Na atoms, as revealed in the partial densities of the phonon states. Thus, the $ThCr_2Si_2$-type structure is unstable, which is further confirmed by no overlap between the Na and S states. On the other hand, for the $CaAl_2Si_2$-type structure, the phonon dispersion curves in the whole Brillouin zone are positive, hence confirming the dynamic stability. There is much overlap between the Na and Fe and the Na and S states, and it is these interactions that stabilize the structure.

Preliminary characterization reveals that $NaFe_{1.6}S_2$ is a magnetic semiconductor without superconductivity even down to 2 K. Presented in Figure S2 is the magnetic susceptibility. As can be seen, an anomaly occurs at $T_a = 205$ K, below which the magnetic susceptibility steeply decreases with decreasing temperature. This transition is clearly seen in the $d(\chi_m T)/dT$ curve and is also confirmed in the heat capacity curve (Figure S3, SI) with a clear λ-type shape peak at $T = 202$ K. Although without a prominent maximum in the $\chi_m - T$ curve, it is likely an antiferromagnetic transition because the $\chi_m - T$ curve around the transition temperature looks so much like those of the alkali intercalated FeSe superconductors whose antiferromagnetic transitions have been confirmed by neutron diffraction.[15] Also, the $\chi_m - H$ curves at 300 and 180 K are linear with little hysteresis because of a possible Fe impurity not detectable by PXRD. Similar antiferromagnetic transitions have also been observed in $Na_2OFe_2Se_2$, $BaOFe_2Se_2$, and $SrMn_2As_2$.[16] The shape of the $\chi_m - T$ curve also reminds us of the spin-crossover transition, as

dx.doi.org/10.1021/ic4016349 | Inorg. Chem. 2013, 52, 12860−12862

reported for metal complexes and thiospinels,[17] but no characteristic plateau was observed in the $\chi_m T-T$ curve (Figure S4, SI). More measurements, such as Mössbauer spectrometry and neutron diffraction, are needed to further clarify the nature of this transition.

The electrical resistivity (Figure S5, SI) reveals semiconducting behavior, with room temperature resistivity of 196 mΩ cm, approximately 4 times that of $K_xFe_{2-y}S_2$.[14] As the temperature is lowered, an anomaly is observed in the temperature range of 140−180 K, well below the characteristic temperature in the χ_m-T curve. Similar behavior was also observed in $SrMn_2As_2$[16c] with antiferromagnetic transition and in iron(II) complexes[18] with spin-crossover transition. The activation energies below and above the anomaly are 0.046 eV (50−100 K) and 0.122 eV (200−300 K), respectively, both indicating a narrow band gap. It should be noted that FeS is a localized spin antiferromagnet with metallic conductivity and is characterized by three phase transitions, one structural transition at T = 420 K, and two magnetic transitions at T = 453 and 600 K, so the FeS impurity in the $NaFe_{1.6}S_2$ sample has no significant effects on the properties.[19]

In conclusion, $NaFe_{1.6}S_2$ was successfully synthesized. It adopts a $CaAl_2Si_2$-type structure, which is dynamically stable, as revealed by first-principles calculations, and is a magnetic semiconductor. It shares many similarities with a $K_xFe_{2-y}Se_2$ superconductor, and the 20% iron vacancies may be one of the reasons responsible for the absence of superconductivity in this compound.[7d,20] Our results not only enrich the structural diversity of the $A_xM_{2-y}X_2$ system but also will shed light on the relationship between the structure and physical properties of this system.

■ ASSOCIATED CONTENT

Supporting Information

Details on the preparation and characterization, first-principles calculation details, comparison of the PXRD patterns for $Na_xFe_{2-y}S_{2+z}$ (Figure S1), magnetic susceptibility (Figure S2), heat capacity (Figure S3), $\chi_m T-T$ curve (Figure S4), resistivity (Figure S5), and X-ray crystallographic data in CIF format for $NaFe_{1.6}S_2$. This material is available free of charge via the Internet at http://pubs.acs.org.

■ AUTHOR INFORMATION

Corresponding Author

*E-mail: chenx29@iphy.ac.cn.

Notes

The authors declare no competing financial interest.

■ ACKNOWLEDGMENTS

This work was financially supported by the National Natural Science Foundation of China under Grants 90922037, 51072226, and 51202286 and the International Center for Diffraction Data. The authors are grateful to Yu Liu and Dandan Li for helpful discussions.

■ REFERENCES

(1) Paglione, J.; Green, R. L. *Nat. Phys.* **2010**, *6*, 645−658.
(2) Lei, H. C.; Wang, K. F.; Hu, R. W.; Ryu, H.; Abeykoon, M.; Bozin, E. S.; Petrovic, C. *Sci. Technol. Adv. Mater.* **2012**, *13*, 054305.
(3) (a) Tapp, J. H.; Tang, Z. J.; Lv, B.; Sasmal, K.; Lorenz, B.; Chu, P. C. W.; Guloy, A. M. *Phys. Rev. B* **2008**, *78*, 060505(R). (b) Rotter, M.; Tegel, M.; Johrendt, D. *Phys. Rev. Lett.* **2008**, *101*, 107006.
(4) (a) Kamihara, Y.; Watanabe, T.; Hirano, M.; Hosono, H. *J. Am. Chem. Soc.* **2008**, *130*, 3296−3297. (b) Matsuishi, S.; Inoue, Y.; Nomura, T.; Yanagi, H.; Hirano, M.; Hosono, H. *J. Am. Chem. Soc.* **2008**, *130*, 14428−14429.
(5) Zhu, X. Y.; Han, F.; Mu, G.; Cheng, P.; Shen, B.; Zeng, B.; Wen, H.-H. *Phys. Rev. B* **2009**, *79*, 220512(R).
(6) (a) Hsu, F. C.; Luo, J. Y.; Yeh, K. W.; Chen, T. K.; Huang, T. W.; Wu, P. M.; Lee, Y. C.; Huang, Y. L.; Chu, Y. Y.; Yan, D. C.; Wu, M. K. *Proc. Natl. Acad. Sci. U.S.A.* **2008**, *105*, 14262−14264. (b) Yeh, K. W.; Huang, T. W.; Huang, Y. L.; Chen, T. K.; Hsu, F. C.; Wu, P. M.; Lee, Y. C.; Chu, Y. Y.; Chen, C. L.; Luo, J. Y.; Yan, D. C.; Wu, M. K. *Europhys. Lett.* **2008**, *84*, 37002.
(7) (a) Guo, J. G.; Jin, S. F.; Wang, G.; Wang, S. C.; Zhu, K. X.; Zhou, T. T.; He, M.; Chen, X. L. *Phys. Rev. B* **2010**, *82*, 180520(R). (b) Wang, A. F.; Ying, J. J.; Yan, Y. J.; Liu, R. H.; Luo, X. G.; Li, Z. Y.; Wang, X. F.; Zhang, M.; Ye, G. J.; Cheng, P.; Xiang, Z. J.; Chen, X. H. *Phys. Rev. B* **2011**, *83*, 060512(R). (c) Maziopa, A. K.; Shermadini, Z.; Pomjakushina, E.; Pomjakushin, V.; Bendele, M.; Amato, A.; Khasanov, R.; Luetkens, H.; Conder, K. *J. Phys.: Condens. Matter* **2011**, *23*, 052203. (d) Fang, M. H.; Wang, H. D.; Dong, C. H.; Li, Z. J.; Feng, C. M.; Chen, J.; Yuan, H. Q. *Europhys. Lett.* **2011**, *94*, 27009. (e) Guo, J. G.; Chen, X. L.; Wang, G.; Jin, S. F.; Zhou, T. T.; Lai, X. F. *Phys. Rev. B* **2012**, *85*, 054507.
(8) (a) Klepp, K. O.; Boller, H. *Monatsh. Chem.* **1978**, *109*, 1049−1057. (b) Sabrowsky, H.; Rosenberg, M.; Welz, D.; Deppe, P.; Schäfer, W. *J. Magn. Magn. Mater.* **1986**, *54*−*57*, 1497−1498. (c) Häggström, L.; Seidel, A. *J. Magn. Magn. Mater.* **1991**, *98*, 37−46. (d) Huan, G.; Greenblatt, M. *J. Less Common Met.* **1989**, *156*, 247−257. (e) Greaney, M.; Huan, G. H.; Ramanujachary, K. V.; Teweldemedhin, Z.; Greenblatt, M. *Solid State Commun.* **1991**, *79*, 803−810. (f) Huan, G.; Greenblatt, M.; Croft, M. *Eur. J. Solid State Inorg. Chem.* **1989**, *26*, 193−220.
(9) Liu, Z. Q.; Fang, A. H.; Huang, F. Q.; Jiang, M. H. arXiv:0808, 1784.
(10) Ying, T. P.; Chen, X. L.; Wang, G.; Jin, S. F.; Zhou, T. T.; Lai, X. F.; Zhang, H.; Wang, W. Y. *Sci. Rep.* **2012**, *2*, 426.
(11) (a) Ying, T. P.; Chen, X. L.; Wang, G.; Jin, S. F.; Lai, X. F.; Zhou, T. T.; Zhang, H.; Shen, S. J.; Wang, W. Y. *J. Am. Chem. Soc.* **2013**, *135*, 2951−2954. (b) Scheidt, E.-W.; Hathwar, V. R.; Schmitz, D.; Dunbar, A.; Scherer, W.; Mayr, F.; Tsurkan, V.; Deisenhofer, J.; Loidl, A. *Eur. Phys. J. B* **2012**, *85*, 279. (c) Lucas, M. B.; Free, D. G.; Sedlmaier, S. J.; Wright, J. D.; Cassidy, S. J.; Hara, Y.; Corkett, A. J.; Lancaster, T.; Baker, P. J.; Blundell, S. J.; Clarke, S. J. *Nat. Mater.* **2013**, *12*, 15−19.
(12) Gladyshevskii, E. I.; Kripyakevich, P. I.; Bodak, O. I. *Ukr. Fiz. Zh.* **1967**, *12*, 447−452.
(13) (a) Bronger, W. *Pure Appl. Chem.* **1985**, *57*, 1363−1372. (b) Bronger, W.; Müller, P. *J. Alloys Compd.* **1997**, *246*, 27−36.
(14) Ying, J. J.; Xiang, Z. J.; Li, Z. Y.; Yan, Y. J.; Zhang, M.; Wang, A. F.; Luo, X. G.; Chen, X. H. *Phys. Rev. B* **2012**, *85*, 054506.
(15) (a) Liu, R. H.; Luo, X. G.; Zhang, M.; Wang, A. F.; Ying, J. J.; Wang, X. F.; Yan, Y. J.; Xiang, Z. J.; Cheng, P.; Ye, G. J.; Li, Z. Y.; Chen, X. H. *Europhys. Lett.* **2011**, *94*, 27008. (b) Ye, F.; Chi, S.; Bao, W.; Wang, X. F.; Ying, J. J.; Chen, X. H.; Wang, H. D.; Dong, C. H.; Fang, M. H. *Phys. Rev. Lett.* **2011**, *107*, 137003.
(16) (a) He, J. B.; Wang, D. M.; Shi, H. L.; Yang, H. X.; Li, J. Q.; Chen, G. F. *Phys. Rev. B* **2011**, *84*, 205212. (b) Han, F.; Wan, X. G.; Shen, B.; Wen, H.-H. *Phys. Rev. B* **2012**, *86*, 014411. (c) Wang, Z. W.; Yang, H. X.; Tian, H. F.; Shi, H. L.; Lu, J. B.; Qin, Y. B.; Wang, Z.; Li, J. Q. *J. Phys. Chem. Solids* **2011**, *72*, 457−459.
(17) (a) Shatruk, M.; Andrasi, A. D.; Chambers, K. E.; Stoian, S. A.; Bominaar, E. L.; Achim, C.; Dunbar, K. R. *J. Am. Chem. Soc.* **2007**, *129*, 6104−6116. (b) Womes, M.; Jumas, J. C. *J. Phys. Chem. Solids* **2013**, *74*, 457−465.
(18) Nihei, M.; Takahashi, N.; Nishikawab, H.; Oshio, H. *Dalton Trans.* **2011**, *40*, 2154−2156.
(19) Horwood, J. L.; Townsend, M. G.; Webster, A. H. *J. Solid State Chem.* **1976**, *17*, 35−42.
(20) Wang, D. M.; He, J. B.; Xia, T.-L.; Chen, G. F. *Phys. Rev. B* **2011**, *83*, 132502.